

A computational study of the molecular and
crystal structure and selected physical properties
of octahydridosilasequioxane, $(\text{Si}_2\text{O}_3\text{H}_2)_4$. Part I.
Electronic and structural properties.

C.J.H. Schutte^a and J.A. Pretorius^b

a Chemistry Department and Centre for Advanced Studies

b Chemistry Department and Supercomputer Centre

University of Pretoria

Hillcrest, Pretoria

South Africa

June 22, 2010

Contents

1	INTRODUCTION	3
2	A brief review of silicate structures	6
3	COMPUTATIONAL PROCEDURES	10
4	Crystal structure of octahydridosilasequioxane	11
4.1	Structural aspects	11
4.2	Hydrogen Interaction	11
4.3	Interactions along the z-axis	12
4.4	Intermolecular Interaction	13
4.5	Problematic aspects of the structure	13
5	Structural optimization	15
6	Molecular orbitals	16
6.1	Disiloxane	16
6.2	Octahydridosilasequioxane O_h	17
6.2.1	Convergence criteria	18
6.2.2	MO energies and symmetries	18
6.2.3	The orbital diagrams	21
6.3	Partial electron charges	23

7 Conclusions **25**

List of Figures

1	The molecular structure of octahydridosilasequioxane	4
2	Schematic representations of the H-atom charge distributions . .	5
3	Partial charge distribution in disiloxane.	6
4	Five bonding types in tetrahedral Si-structures	8
5	Trifurcated Hydrogen interactions	12
6	Hydrogen interactions of the octahydridosilasequioxane molecules	13
7	Molecular repeating unit octahydridosilasequioxane	14
8	MOs 13, 14, 15 and 16 of disiloxane	18
9	MOs 21, 22 and 22 of disiloxane	19
10	The highest orbitals 106 107, 108, 109 of octahydridosilasequioxane	21
11	MOs 102, 103, 104 and 105	22
12	MOs 77, 80, 82 and 88 within central cavity	24
13	Two of the members of the triply-degenerate set MOs 83-85) . .	25

List of Tables

1	Bond and electron density properties of silicates	32
2	Computed structural and electron density data	33

(June 22, 2010)

Abstract

The free molecule octahydridosilasequioxane, $\text{Si}_8\text{O}_{12}\text{H}_8$, was computationally studied, as well as embedded in the unit cell. The point group of the free molecule is indeed O_h and its crystal symmetry is reduced to C_{3i} , thus confirming the occurrence of two different types of Si-O-Si bond lengths found experimentally. The molecular orbitals of the free molecule show that some electron density occurs in the cubic cavity, thus contributing to the opening of the Si-O-Si angle. A study of the packing in the unit cell identifies a new type of packing scheme in which eight (partial) molecules participate: each apex H-atom of one protruding Si-H bond of every molecule points to the corner of an *equilateral* triangle having 2.631 Å sides. All hydrogen atoms in both the free molecule and in the solid state carry negative partial charges. The reason for this is also explored, as well as its consequences for the unique packing scheme.

Keywords

octahydridosilasequioxane, disiloxane, disilyl ether, octaspherosiloxane, tetrahydroxysilicon, virial ratio, infra-red, raman, phonon, atomic polar tensor, electron density

Abbreviations

MO – Molecular Orbital, AO – Atomic Orbital, DFT – Density Functional Theory, APT - Atomic Polar Tensor, SMP – Shared Memory Processor, G03 – GAUSSIAN 03, PAW - Projector Augmented Wave method

1 INTRODUCTION

Silicon oxide compounds play an important role in nature, science and technology and lately this role has even been extended into the biochemical field, where it has been shown that silicon-like precipitates occur in the brain near neurons which have been damaged by Parkinson's disease (Birchall and Chappell 1988; Bilinski *et al.* 1992); the nature of these aluminosilicates has not yet been determined, despite extensive efforts.

With respect to SiO_2 it is of interest to note the developments around the ZSM-5 (MFI framework) Zeolite Mobil catalyst (Owen *et al.* 1985, and references therein). Early demonstration processes effectively produced ethene and light olefins as a gasoline fraction from methanol through the MTO (Methanol to Olefin) process by AECI, South Africa in 1982 (Seddon 2006) and the MTG (Methanol to Gasoline) process at Montonui in New Zealand (1985). This was followed by the joint development by United Oil Production (UOP) and Norsk Hydro, the UOP/HYDRO process, utilizing a silica aluminophosphate (SAPO-34) catalyst (Vora *et al.* 1997), having a framework structure similar to ZSM-5, but now exhibiting higher molecular shape-selectivity for production of ethylene and propylene from methanol (Wilson *et al.* 1999). The highly selective nature of a few SiO_2 -based Zeolite catalysts (referred to above), also considering their shape selective capacities, is indicative of a subtle underlying electron distribution.

In the light of the ubiquitous presence of silicon-oxygen compounds in science, technology and nature, it is therefore important to arrive at a better understanding of the electron distributions in such molecules. Equally important are those silica compounds that have hydrogen atoms protruding from the Si-sites, which not only could influence crystalline packing schemes by their perturbing effect on the electron distribution in a macro-molecule, but could also influence the course of a chemical reaction or adsorption/catalytic process.

Some crystallographic work on the electron-density in silicates has been done (Sasaki *et al.* 1982), but so far there has been no correlation between the experimental electron densities and computed values. One of the reasons for this unsatisfactory state of affairs is the fact that most silicon compounds occur in nature as infinite 1D, 2D and 3D-oligomers, which contribute to make this kind of computation intractable. In trying to resolve this dilemma, we focused on the octahydridosilasequioxane molecule (see Figure 1), which is large enough to allow general conclusions about the nature of S-O and H-Si-O bonds to be drawn, but yet small enough to be subjected to high-level chemical computations. Also of special importance is the up-to-now inexplicable variation of Si-O-Si bond angles, which is addressed in this study, and which must have its origin in the variation of the electron distributions in such molecules.

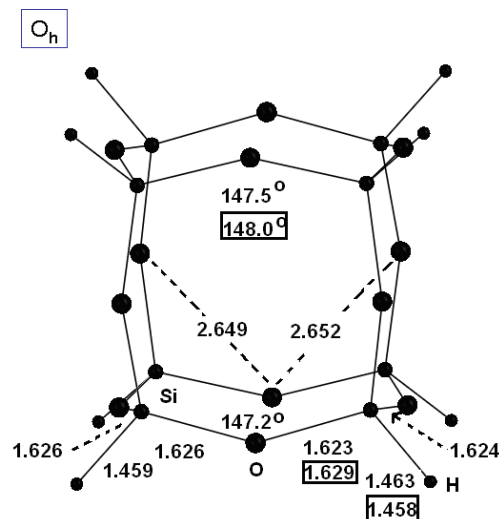


Figure 1: The molecular structure of the octahedral molecule octahydridosilasequioxane as determined in the neutron-diffraction study of Törnroos (1994). The dots at the corners are silicon atoms, the dots in the centre of the edges are oxygen atoms, while the atoms protruding from the corner silicon atoms, represent hydrogen atoms. The partial charges on the atoms are discussed below. The numbers in squares refer to the computed [G03] Si-O and Si-H interatomic distances. The two crystallographically different Si-O distances are important. More data are summarized in Tables 1 and 2.

The importance of understanding the factors that contribute to the unusual stability of the cubic-octameric silsesquioxanes (sometimes also known under the acronym COSS) is underlined by the up-surfing interest in the synthesis of COSS basic structures, in which the peripherally-protruding H-atoms are replaced by eight organic and, in some cases, by biological fragments (Heyl *et al.* 2010). Organic and biological fragments can be introduced under mild conditions into the COSS skeleton, such as the azidopropyl-group, but the reaction mechanism has not yet been established. Our computational studies could enhance such mechanistic and structural studies, the more so, since it has been established that organic COSS-molecules are biocompatible - and might thus form the basis for the exploration of new medicines.

The molecules silane SiH_4 (Figure 2), tetrahydroxysilicon(IV) $\text{Si}(\text{OH})_4$ (Figure 2) and disiloxane (disilyl ether) $\text{SiH}_3 \cdot \text{O} \cdot \text{SiH}_3$ (Figure 3) are used as "reference compounds" in this paper; their computed atomic fractional charges (Mulliken and APT, see below) are displayed in Figures 2 and 3 respectively, showing a large partial-charge variation on the respective atoms.

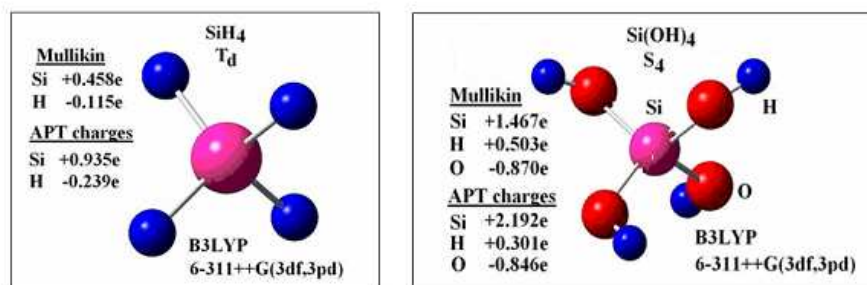


Figure 2: Schematic representations of the H-atom charge distributions in the *optimized* SiH_4 and $\text{Si}(\text{OH})_4$ *free molecules*, calculated computationally as discussed below.

We aim to investigate the following aspects of the octahydridosilasequioxane molecule using advanced computational methods to explore following aspects:

1. The symmetry of the optimized free molecule, its geometry and its electronic structure.
2. The implications of a negative fractional charge on hydrogen atoms on the structures of some simple silicon compounds, and more specifically, in the octahedral molecule octahydridosilasequioxane (Figure 1) with its "spiky" appearance.
3. The experimentally determined crystal structure of the solid state compared with that of the computed optimized crystal structure.
4. The partial (Mulliken and APT) charges on all the atoms.

(June 22, 2010)

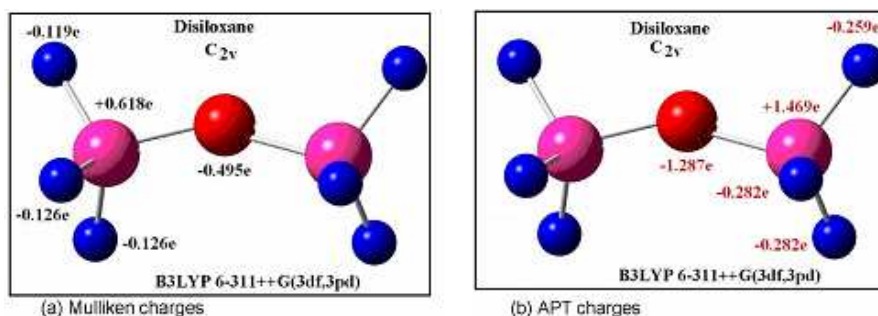


Figure 3: The partial charge distribution in the optimized disiloxane molecule. Figure (a) deploys the Mulliken partial charges and in Figure (b) the APT charges are shown. More data are shown in Tables 1 and 2.

5. The vibrational modes and frequencies of the crystal cluster vibrations, so that packing forces in the solid state may be determined.
6. Decide which type of electron-charge density (Mulliken or APT) is suitable for modeling this type of silicates.

The results obtained in this study correlate well with experimental results and electron densities so that this octahydrosilasequioxane can be considered to be representative of silicates and as such contribute to the knowledge of silicate structures and their reactivity in general. The vibrational structure of the free molecule and when embedded in the crystal lattice is reported in Paper II (Schutte and Pretorius 2010).

2 A brief review of silicate structures

Molecules which contain one or more Si-H chemical bonds in which a hydrogen atom is *directly* bonded to a silicon atom display interesting charge distributions, especially when silicon is also bonded to an oxygen atom. Since hydrogen is slightly more electronegative than silicon (2.1 versus 1.8) on the Pauling scale (Pauling 1960), it should accumulate a small fractional negative charge when bonded to a silicon atom - unless the charge distribution is very much perturbed when one or more strong electronegative atoms or groups are present, such as oxygen or hydroxyl ions, which satisfy the other available valencies of silicon.

The molecule Si(OH)₄ can be considered to be the parent compound of all silicate types, which are formed by the removal of water molecules from two or more such molecules, followed by bond rearrangements. Since this paper concerns itself with computational aspects of the structural, chemical bonding, electronic and the spectroscopic properties of some types of *tetrahedral* Si-compounds, it is necessary to give a brief review of the various structures formally derived from Si(OH)₄ in order to arrive at a new classification of silicate structures.

(June 22, 2010)

It is pointed out that the present paper makes no reference to (distorted) octahedrally-coordinated SiO_6 groups that occur in silicates, containing small cations which compete with the Si for the oxygen. Only a few such examples have been found, in which the nature of the chemical bonds are quite different from that of tetrahedrally-coordinated bonds around Si. The average Si-O bond length in such compounds is 1.77 Å (ranging from 1.70 Å to 1.84 Å, see Mak & Zhou 1992; p.300), compared with the tetrahedral average of about 1.62 Å.

The crystallographically-determined charges on the atoms in $\text{K}_2\text{Si}^{VI}\text{Si}_3^{IV}\text{O}_9$ are +3.32e on Si^{VI} , +2.5e on Si^{IV} and -1.4e on O, as determined by Swanson & Prewitt (1983). The electron densities of Swanson and Prewitt (1983) for Si^{IV} and O are in the same ball park as that found computationally for octahydrdidosilasequioxane discussed below, notwithstanding possible structural perturbations exerted in the octahedral molecule. It is, therefore, necessary to give a brief overview of the electronic structure and geometry of the silicates, as well of their classification, which is specially adapted for this investigation.

Those silicon-oxygen compounds containing one or more *tetrahedral* Si-O-Si sequences are collectively known as *silicates* (Cotton & Wilkinson 1988), the structures of which may consist of the following types:

- **1D ionic chains:** Accurate X-ray and neutron diffraction electron density and structural data are available for the ionic-chain entity occurring in ortho-enstatite, MgSiO_3 , sometimes written as $\text{Mg}_2(\text{SiO}_3)_2$ (Sasaki *et al.* 1982). Ionic chains are also observed in the synthetic metasilicate, Na_2SiO_3 sodium pyroxene, containing a single chain of SiO_4 tetrahedra sharing an apex oxygen atom (McDonald & Cruickshank 1967). The compound $\text{NaTiSi}_2\text{O}_6$ might even consist of a haldane spin-1 chain system and not as a quasi one-D chain system as found by other workers (Popović, Sljivancanin and Vukaljević 2004); this article was commented upon, by Streltsov, Popova & Khomskii (2006).
- **2D planar ionic nets:** These nets occur for instance in $\beta\text{-Na}_2\text{Si}_2\text{O}_5$ (Pant 1968).
- **3D ionic lattices:** Forming concatenated $(-\text{O-Si-O-Si-})_n$ networks, where $n = 1, 2, 3$, as well as cyclic ionic structures, see for example beryl, $\text{Be}_3\text{Al}_2\text{Si}_6\text{O}_{18}$ (Morosin 1972) and even in ionic cages (Knight, Kirkpatrick & Oldfield 1986).

However, for the computational and bonding purposes of the present paper, it is more convenient not to use the many different chemical and topological descriptions of silicate structures found in the literature (Wells 1984, for Si-O-Si angles of up to almost 180°; Mak & Zhou 1992), but to classify tetrahedral Si-compounds (see Liebau 1985) according to a *simplified* set of *five basic structures* as displayed in Figure 4. This set of five bonding types may be used to describe the structures of a wide variety of tetrahedral Si-compounds, varying from organosilicon compounds, through quartz and all modifications of SiC, to that of very complex inorganic silicates.

(June 22, 2010)

The individual members of this set of basic structural types exhibit many common physical properties, although there are some large variations in other properties, such as, the value of the Si-O-Si bond angle in Types II to V of Figure 4 (see also Wells 1984). The reasons for this variation have never been satisfactorily explained by means of computations.

This paper specializes in the following cases of Types I to V (see Figure 4):

1. Where *only another Si-atom* is allowed to bond to any one of the oxygen atoms, although it is possible to attach almost any type of atom to the oxygen atoms, as, for instance, in the *zeolites*, in which AlO_4 tetrahedra alternate with SiO_4 tetrahedra, sharing an oxygen atom between them.
2. Where $\{W, X, Y, Z\} = \text{H}$ in Types I, II and IV molecules, since hydrogen is a good chain-terminating group, contributing only one electron to the electron pool of a molecule (stabilizing the underlying electronic structure and eliminating any dangling bonds on the silicate surface, keeping the molecule in a spin state with $S = 1$), thus simplifying any computation without introducing too large bond polarisations due to electronegativity differences.

Octahydridosilasequioxane exhibits Type IV structure and can serve as a prototype for a computational study of all five structural types, especially when the study is *enhanced* with a study of Type I molecules (silane, SiH_4 and $\text{Si}(\text{OH})_4$, see Figure 2) and a Type II molecule (disiloxane, $\text{SiH}_3\cdot\text{O}\cdot\text{SiH}_3$, see Figure 3) as reported in this paper.

Octahydridosilasequioxane is *small enough* to be amenable to high-level computational studies to investigate the structural properties, electronic structure and spectroscopy of the hypothetical isolated molecule, as well as in the crystal unit cell; it is *large enough* to serve as a non-trivial example of a typical silicate structure, allowing some important generalized conclusions to be drawn about silicate structures of Types I to IV. The computational methodology and basis set used here may serve as a model for computing properties of other silicate units.

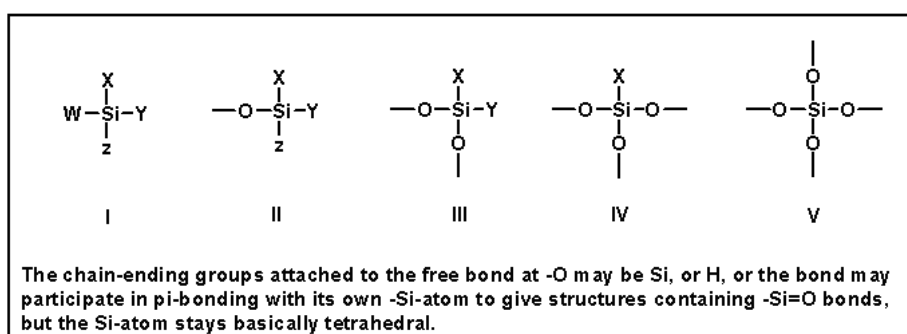


Figure 4: The Five bonding types in tetrahedral Si-structures used in this paper.

(June 22, 2010)

Octahydridosilasequioxane, $\text{Si}_8\text{H}_8\text{O}_{12}$, is a member of a homologous series of cage-like molecules with the simplest empirical formula given as $(\text{SiHO}_{1.5})_n$ with n even and $n > 4$. Members with $n = 8, 12, 14, 16, 18$ were synthesized and characterized by Agaskar (1991) and Agaskar and Klemperer (1995), displaying other symmetries, such as D_{5h} , D_{3h} and D_{2d} . These papers also report some IR bands (Nujol mull between KBr plates) of octahydridosilasequioxane occurring at 2290 (s), 1140 (vs), 918 (w), 885 (sh), 870 (s), 500 (sh), 470 (w), 395 (m) cm^{-1} ; these are unambiguously assigned below. The paucity of bands occurring in the experimental IR spectrum needs to be theoretically explained, seeing that the site group symmetry of the molecule might be lower than the expected octahedral symmetry. In addition there seems to be no spitting in the solid state caused by intermolecular coupling and this curious fact also needs to be investigated.

Ideally, the Si-atoms in the $\text{Si}_2\text{O}_3\text{H}_2$ repeating unit illustrated Figure 7, should form four single tetrahedral covalent bonds with interbond angles of around 109° . In practice, however, the Si-O-Si bond is bent open and we enquire about the reasons for this. The oxygen atoms in the Si-O-Si sequence should also exemplify single Si-O bonds; the ideal Si-O-Si interbond angle should therefore be around 105° as in water. It is however, instructive to briefly review some general structural data pertaining to particular parts of the repeating unit $\text{Si}_2\text{O}_3\text{H}_2$ shown above:

Organic structures containing Si-O-Si bond sequences: The Si-O average bond length in X-Si-O-Si-X compounds, where X is an organic group, fall in the narrow range of $1.622 \pm 0.014 \text{ \AA}$ for a total of 70 different molecules (the upper quartile is 1.646 \AA , while the lower quartile 1.617 \AA); data from Lide (2009-2010). However, the X-O-X interbond angle in such compounds displays a wide variation, ranging from about 90° to almost 180° , depending upon the nature, size and electronegativity of the groups X (Bailar *et al.* 1973).

Structures containing single S-H-bonds: The Si-H bond length in SiH_4 is $1.4707(6) \text{ \AA}$ and for $\text{Si}_2\text{H}_6(\text{g})$ it is $1.4874(17) \text{ \AA}$ (Kuchitsu 1998).

Inorganic silicates: The Si-O bond in quartz $\text{SiO}_2(\text{s})$ is formally a single bond, but its length depends upon the crystal modification. In α -quartz there are two crystallographically different Si-O distances of 1.608 and 1.610 \AA (Bailar *et al.* 1973), respectively. In β -quartz the Si-O bond length is 1.58 \AA , while the Si-O-Si bond angle is 155° (Wright & Lehmann 1981; Dusek *et al.* 2001), leading to a less distorted structure.

An X-ray electron-density map shows that the Si-atom in β -quartz has a charge of $+1.22e$ while the O-atom carries a charge of $-0.61e$ (Mak & Zhou 1992; Tucker, Keen & Dive 2001). The Si-atom is formally tetrahedrally hybridized in inorganic silicates, but the Si-O-Si interbond angle is usually around 140° .

The mean atom charges from electron-density maps in the *silicates* are, for instance, in $\text{Mg}_2[\text{SiO}_3]_2$: Mg $+1.82e$, Si $+2.28e$, O-terminal $-1.42e$ and O-

(June 22, 2010)

bridging $-1.27e$ (Sasaki *et al.* 1982), showing that some charge transfer takes place between the Si and the O-atoms (Pauling electronegativity of Si is 1.8, while that of H and O are 2.1 and 3.5, respectively), see Pauling (1960). These data are summarized in Table 1

3 COMPUTATIONAL PROCEDURES

All computations on *isolated molecules* were carried out on an IBM computer-cluster with a pre-compiled set of *Gaussian-03* programs (GAUSSIAN 03, 2004), configured for parallel computing under Power LINUX (SUSE 10.2). Default settings for Gaussian-03 were used as described in the manual (Frisch, Frish & Trucks). More details about the computational methodology can be found in Hirst (1990); Kohanoff (2006); Foresman & Frisch (1998), as well as in original references cited in the Gaussian Manual. All molecular structural and spectroscopic illustrations were done with the program *GaussView* (2007), while graphs were drawn with the Program *Origin* (Ver. 7.5). Crystal structure data were visualized from CIF files with the program *Mercury* (Ver. 2.0) of the Cambridge Crystallographic Data Centre (CCDC).

The default settings of Gaussian G03 were used for all calculations on *free molecules*, except when otherwise indicated. A big basis set was chosen for all computations, namely 6-311++G(3df,3pd), together with the DFT B3LYP computational methodology. Optimization computations were done first, followed by frequency calculations in all cases, to ensure that the reported structures are determined at potential-energy minima and not at saddle points, except for the cluster containing eight octahydridosilasequioxane molecules, which is too large for our cluster to handle. *No imaginary frequencies for octahedral octahydridosilasequioxane were found in the Gaussian computations.*

Attention is especially drawn to the fact that the so-called "molecular orbitals" obtained from DFT calculations, using the B3LYP *functional*, are not to be considered to be "DFT molecular orbitals", since the GAUSSIAN program G03 defaults to calculate the SCF orbitals at the optimized geometry. This is especially true for the pictorial representations of electron density, which are usually called "molecular orbitals" and all the drawings of such orbitals in this paper (for instance, Figure 8) are actually SCF-orbitals.

All electronic structural computations for the *solid state* were carried out on the INTEL architecture of the IBM cluster executing in parallel, using the MedeA (Ver. 2.0.3.2, 2006) set of programs, with special reference to the programs VASP (Ver. 4.6) (Kresse & Furthmüller 1996a,b; Kresse & Joubert 1999) for crystal structure optimizations and PHONON (MedeA: Phonon 2003), for phonon dispersions and phonon densities of states along the special directions of the reciprocal lattice. The software sets available within the MedeA-Suite were used to produce the illustrations from the extensive set of data generated for each run. For the VASP software parameters, the GGA-PBE potential approximation were used on a full structural optimization (relaxed atom positions only) with PAW plane wave cutoff of 240 eV, refined as a non-magnetic entity

and at a SCF k -point spacing of 0.3 Å.

4 Crystal structure of octahydridosilasequioxane

4.1 Structural aspects

The compound octahydridosilasequioxane, $\text{Si}_8\text{H}_8\text{O}_{12}$, (it is sometimes colloquially called *octaspherosiloxane*, the name referring to its almost spherical O_h -shape), is one of the most interesting silicates that has Si-H bonds. The molecule can be considered to be a three-dimensional octahedral polymer; its experimentally-determined molecular structure is diagrammatically shown in Figure 1 (Larsson 1960; Törnroos 1994). The structure of the repeating unit can symbolically be generated by condensing together four units of the molecular repeating unit, $(\text{Si}_2\text{O}_3\text{H}_2)$ shown in Figure 7.

The crystal structure of octahydridosilasequioxane was determined by Larsson (1960) as trigonal, who found that it belonged to space group (Nr. 148) $R\bar{3}h$ of $R\bar{3}$, $Z = 3$, $a = 9.131 \pm 0.01$ Å, $b = 9.131 \pm 0.01$ Å, $c = 15.357 \pm 0.015$ Å, $\alpha = 90. \pm 0.0^\circ$, $\beta = 90. \pm 0.0^\circ$ and $\gamma = 120. \pm 0.0^\circ$. The structure was re-determined by Törnroos (1994) by neutron diffraction, *inter alia* yielding better data for the hydrogen atom positions; this structure is shown in Figure 1. The Törnroos space group (Nr. 148, $R\bar{3}$, C_{3i}^2 , $Z = 3$) is the same as that of Larsson (1960), with more accurate lattice parameters, namely: $a = 9.053 \pm 0.001$ Å, $b = 9.053 \pm 0.001$ Å and $c = 15.149 \pm 0.001$ Å (Törnroos 1994). In the Törnroos unit cell the molecule has $C_{3i} = S_6$ site symmetry (Hahn [*Editor*] 2005). One of the most conspicuous features is that the molecular unit does not quite possess O_h -symmetry, since one Si-O bridging bond type is just dissimilar from the other two within the accuracy of the determination.

Törnroos (1994) speculates that, although the crystallographic (site) symmetry of the molecule in the space group $R\bar{3}$ is actually $C_{3i} = S_6$, it is very near to having a *non-crystallographic symmetry* of a much higher point group, namely T_h . If this were true, it would not only lead to a completely different vibrational symmetry analysis of the unit cell, since the non-crystallographic symmetry would then be almost equal to that of the molecular symmetry and the spectroscopic analysis would lead to a different pattern of active vibrations. It would also lead to the question whether the space group is not higher than trigonal. These possibilities are examined below.

4.2 Hydrogen Interaction

$\text{H} \cdots \text{H}$ interactions between the two sets of three (partial) $\text{Si}_8\text{H}_{12}\text{O}_8$ molecules in the unit cell, seem to play an important role in the packing of the molecules in the crystal. Two parallel equilateral triangles of $\text{H} \cdots \text{H}$ side length 2.631 Å, form between adjacent molecules in the same unit cell. *Two hydrogen atoms* (along one Si-O-Si bonding edge) from each molecule are sharing (orthogonally) in the

(June 22, 2010)

triangular hydrogen interactions with the three nearest neighboring molecules in a typical bi-pyramidal arrangement. The parallel triangles are in turn, parallel to the ab -plane or the $[00x]$ Miller plane.

These triangular hydrogen interactions are centered around crystallographic 3-fold rotational symmetry centres (located at: $(\frac{1}{2}\frac{2}{3}z)$ and $(\frac{2}{3}\frac{1}{3}z)$), which implies that these interactions should constitute one of the major packing forces in the solid-state. This is illustrated in Figure 5. The perpendicular distance between the interacting H-atom of the one molecule to the centre of the triangle formed by three other H-atoms is just 2.29 Å. The distance between the H-atom on the equilateral triangle is 2.671 Å. The planes of the triangles, which have the *local symmetry of the site group*, $C_{3i} = S_6$ are just 2.27 Å apart (see also Figure 6 for another view), that is, it is considerably smaller than that customarily assigned to a hydrogen bond. It is clear that these trifurcated hydrogen interactions determine the packing of the molecules in the unit cell and hence, that of the crystal structure; this novel packing scheme is pointed out here for the first time.

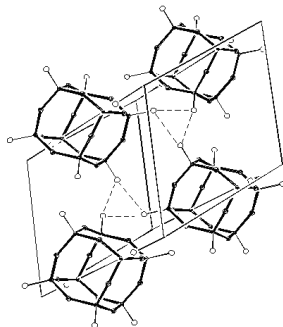


Figure 5: Trifurcated Hydrogen interactions between the triangular arrangement of the apex hydrogen atoms of three octahydridosilasequioxane molecules in the unit cell, at distances of 2.631 Å in the $[001]$ plane. Further details of the packing are shown in Figure 6.

4.3 Interactions along the z-axis

A strong interaction exists between layers of “interstitial” molecules and the triangular H...H interactions (described above). These interactions are along the z-axis at distances of 2.29 Å from the triangular H...H network, establishing a total repeating distance of 12.86 Å between subsequent triangular H...H networks. This is illustrated in Figures refFigure-5 and 6. The role that these hydrogens play in the lattice is further analyzed below.

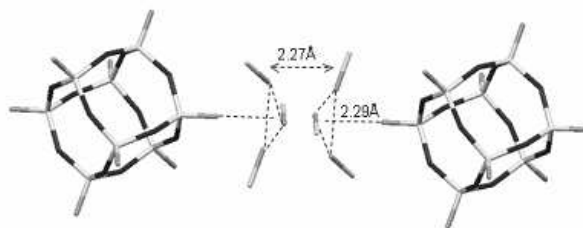


Figure 6: Hydrogen interactions of the octahydridosilasequioxane molecules, orthogonally (along the crystallographic c -axis) with the triangular interactions in the ab -plane. Only the apex Si-H fragments is shown for the six octahydridosilasequioxane molecules contributing to the triangular hydrogen interactions.

4.4 Intermolecular Interaction

The nearest $O \cdots O$ distances between the molecules in the lattice form a zigzag chain (also parallel to the ab -plane) consisting of alternating 4.491 and 4.038 Å distances. The nearest intermolecular $H \cdots O$ distances are 3.254 Å, too far away to speak of meaningful hydrogen bonds. The nearest *intermolecular* $Si \cdots H$ distance is 3.462 Å, while the nearest *intramolecular* distance $O \cdots H$ is 2.512 Å, but the three O-Si-H angles around a Si-atom are not distorted by this balanced pair of internal H-bonds and remain tetrahedral.

Summarizing, it can be surmised that the spiky character of the silicate cube formed by the protruding H-atoms from the surface, seems to contribute very much to the packing forces in this lattice. It is *inter alia* the aim of this study to determine whether this is indeed true, as well as the causes for it.

4.5 Problematic aspects of the structure

The description of the crystal and molecular structure of octahydridosilasequioxane given above reveals some puzzling aspects that we wish to clarify by a computationally exploration of the structure, comparing and contrasting the results with those of the chosen reference compounds. We summarize them as follows, at the same time pointing out that answers to them have wider structural implications for other silicates:

1. Why are the Si-O-Si angles in such cyclic silicates not smaller than the observed $\sim 144^\circ$ (Törnroos 1994), or, put in another way, why are the oxygen atoms, as it were, pushed *outwards* away along the central diagonal planes, such as $(\frac{1}{2} \frac{1}{2} 0)$ from the central open space of the octahedral hollow molecule? If they are indeed pushed outwards, "what" is pushing them?
2. Why are the octahydridosilasequioxane molecules packed together in a unique way in the unit cell? A set of three closely-packed apex hydrogen atoms from three different molecules, arranged in a triangular pattern, to

(June 22, 2010)

establish the packing scheme found in the crystal (see Figures 5 and 6). In this way the molecular symmetry is reduced from O_h in the free molecule to $C_{3i} = S_6$ in the crystal.

3. The close proximity of the sets of triangularly-packed hydrogen atoms in the unit cell raises the question: What are the partial charges on these hydrogen atoms? We have already pointed out that the electronegativity difference between the Si and H-atoms should lead to a partial negative charge on them. Does this packing then occur in spite of the fact that they are all partially negatively-charged? If they are negatively-charged does it mean that the molecule should exhibit an almost Faraday cage-like effect that would influence its chemical and physical reactivity and its tendency not to engage in reactions that produce further typical silicate 3D-networks (see (Nyman *et al.* 1993)?
4. Does the curious contradiction between the paucity of the IR bands occurring in the spectrum of the solid state and the expected 78 vibrational modes yield further information about the site symmetry of the molecule? Furthermore, can the fact that the spectrum shows no sign of intermolecular coupling be related to the packing scheme?

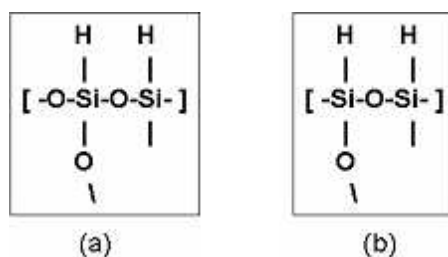


Figure 7: a) Molecular repeating unit of the free octahydridosilasequioxane molecule $(Si_2H_2O_3)_4$. b) Crystallographic asymmetric unit in the octahydridosilasequioxane crystal structure.

These questions are raised here for the first time and prompted us to launch a full-scale computational investigation of both the free molecule and in the solid state. We therefore computationally explore the molecular and electronic structure and the normal vibrational modes and spectra of the three free molecules (Figure 2 and 3) that we chose as reference compounds, as well as those of the molecule octahydridosilasequioxane in the solid state, perturbed by the crystal fields of surrounding molecules in order to compare and contrast their molecular parameters.

5 Structural optimization

Calculations on the isolated *free molecule* octahydridosilasequioxane using the large basis set 6-311++G(3df,3pd) and employing DFT B3LYP computational methodology confirm that it has O_h -symmetry as displayed in Figure 3. The relevant optimized structural and electron-density data are displayed in Table 2, in which they are compared and contrasted with computed and experimental data of the reference compounds silane $\text{SiH}_4(\text{g})$ (Kuchitsu 1998, p68) and disilyl oxide or disiloxane $\text{H}_3\text{Si}\cdot\text{O}\cdot\text{SiH}_3(\text{g})$, (Almenningen *et al.* 1963; Aronson *et al.* 1960; Taga *et al.* 2006; Lord *et al.* 1956; Csonka & Réffy 1994; Needels *et al.* 1991a,b and Wolfe *et al.* 1991) with $\text{Si-O} = 1.64 \text{ \AA}$, $\angle\text{Si-O-Si} = 140^\circ$.

The computed Si-H bond distances in $\text{SiH}_4(\text{g})$ and in the most stable conformation (C_{2v} -symmetry) of $\text{H}_3\text{Si}\cdot\text{O}\cdot\text{SiH}_3$ agree within experimental error with that found experimentally (Kuchitsu 1998). The one Si-H computed distance of the conformation of $\text{H}_3\text{Si}\cdot\text{O}\cdot\text{SiH}_3(\text{g})$ with C_{2v} -symmetry differs 0.004 \AA from those of the other two, in conformance with the symmetry of the molecule; this difference is not found in the experimental data.

The computed Si-O distance for $\text{H}_3\text{Si}\cdot\text{O}\cdot\text{SiH}_3(\text{g})$ agrees with that found experimentally. These results signify the appropriateness of the computational methodology used in this study, together with the chosen basis set as described above.

Table 2 also compares and contrasts three sets of geometrical data, namely:

1. The G03-optimized geometry of the free octahedral octahydridosilasequioxane molecule, $(\text{Si}_2\text{O}_3\text{H}_2)_4$, using the same methodology and basis set.
2. The geometry of the molecule in the solid state as experimentally found by neutron diffraction.
3. The solid state geometry found by unrestrainedly optimizing both the experimentally-obtained unit cell, as well as the structural optimized crystal geometry within the unit cell by the MedeA-suite of programs described above. Most importantly, it is found that the geometrical data of the computed structure with O_h -symmetry agrees within experimental error with the experimentally-obtained structural data in the solid state. The only exception being the non-bonded $\text{O}\cdots\text{O}$ distance in the O_h -structure, which is equal to the arithmetical average of the two solid state $\text{O}\cdots\text{O}$ distances within 0.01 \AA , signifying the effect of the reduction in molecular symmetry from O_h to that of the site symmetry C_{3i} .

This again emphasizes the appropriateness of the two electronic structure computational approaches (G03 and MedeA) used in this study. Both approaches provide optimized structures which are very near to that of the experimental geometry as shown by the data in Table 2.

The *MedeA-VASP* optimization of the solid structure did not change the space group ($R\bar{3}h$ of $R\bar{3}$, Nr. 148) of the compound, although it relaxed the

(June 22, 2010)

linear dimensions of the unit cell somewhat; it even corroborates the correctness of the two different non-bonded O...O distances in the experimentally determined structure, as well as the effect of reducing the molecular symmetry from octahedral to that of the site group C_{3i} .

The main reason for the small elongation of the linear dimensions of the unit cell by the *MedeA-VASP* optimization is found in the opening up of the Si-O-Si-angle from $\sim 147^\circ$ by about 5 to 10° , respectively, together with the lengthening of the non-bonded O...O-distances by about 0.3 Å. The reason for this might be that the *MedeA-VASP* calculation under-emphasizes the extent of the charge transfer taking place between Si and O when they form a specific Si-O bond in a molecule (see discussion below) and hence delivers a slightly more open Si-O-Si bond with slightly longer S-O-distances.

6 Molecular orbitals

6.1 Disiloxane

For the understanding of the molecular structure and the molecular orbitals (MOs) of the free octahydridosilasequioxane molecule discussed below, it is first necessary to study the MOs of the closely-related molecule disiloxane. This molecule can also be regarded as a parent molecule from which all silicate compounds are conceptually constructed by removing two hydrogen *atoms* from each Si-atom and rebinding the two free tetrahedral valencies with the free valencies of other similar $=(\text{H})\text{Si-O-Si}(\text{H})=$ groups, creating an infinite variety of 3D silicate networks. The octahydridosilasequioxane molecule can be considered to be a direct conceptual multiple of disiloxane deprived of four hydrogens.

The classification and description of the molecular orbitals (MOs) of the C_{2v} -optimized molecule disiloxane is important for the understanding of the electronic structure of the molecule. A first classification is arrived at by comparing the energies of the MOs listed above with the ground state energies of the individual AOs of the atoms constituting the molecule (computed using the same G03-methodology and bases sets), as well as by the shapes of the computed orbitals of the equilibrium molecular geometry as discussed below.

In the disiloxane molecule the following electron contributions apply:

1. Two Si-atoms contribute to 28 electrons from the following atomic orbitals (AOs):
 $2(1s^2) = 4e$, $2(2s^2) = 4e$, $2(2p^6) = 12e$, $2(3s^2) = 4e$ and $2(3p^2) = 4e$
2. One O-atom contributing 8 electrons in total from the following orbitals:
 $(1s^2) = 2e$, $(2s^2) = 2e$, $(2p^2) = 2e$
3. Six H-atoms contributing 6e in total from the one orbital each, viz. $6(1s^1) = 6e$.

The total number of electrons is thus 42, built up from individual AOs that form 21 occupied MOs, all of the non-degenerate σ -type. The electronic state is 1A_1 .

A comparison of energies of the MOs at the equilibrium C_{2v} -optimized structure of the octahydridosilasequioxane, $\text{Si}_8\text{H}_8\text{O}_{12}$ molecule and the computed

(June 22, 2010)

energies and symmetries for the AOs of the separate constituting atoms Si, O and H immediately yields the following information regarding the lower set of MOs (G03 computed MO symmetries and energies in hartree are listed in round brackets):

(a) **Occupied MOs remaining almost pure AOs:**

1. **MOs 1 and 2:** (-66.12113 B_2) (-66.12113 A_1) 4e in almost pure Si $1s^2$ AO at -66.14313 hartree.
2. **MO 3:** (-19.12964 A_1) 2e in almost pure O $1s^2$ AO at -19.27791 hartree.
3. **MOs 4 to 5:** (-5.29109 B_2) (-5.29107 A_1) 4e from almost pure Si $2s^2$ AO at -5.30865 hartree.
4. **MOs 6 to 11:** (-3.65086 A_1) (-3.65085 B_2) (-3.64862 B_1) (-3.64862 A_2) (-3.64858 A_1) (-3.64857 B_2) 12e from the set of 12 Si $2p^6$ AOs at -3.67014, -3.66687, -3.66687 hartree.

(b) **Occupied orbitals forming proper MOs:**

MOs 12 to 21: There are 18 electrons in 9 doubly occupied MOs from the outer shells AOs of Si, O and H at the following computed values:

[Si $3s^2$ (-0.45591) + Si $3p^2$ (-0.19417) + O $2p^2$ (0.39164) + H $1s^1$ (-0.50226)]

giving rise to MOs of the following symmetries:

(-1.00400 A_1) (-0.60135 B_2) (-0.51057 A_1) (-0.43954 B_2) (-0.41702 A_1) (-0.41608 B_1) (-0.35402 B_2) (-0.35353 A_2) (-0.31706 A_1) (-0.31381 B_1)

A huge decrease in energy is observed going from the respective AOs to the MOs, showing the extent of the electronic interaction when the MOs are formed. Hydrogen atoms play a large role in the MO-structure. These MOs are the proper molecular orbitals of the LCAO theory and are further discussed below, together with their SCF orbital electron density plots (colloquially called "orbital shapes").

(c) **Virtual orbitals 22 - 24:**

The first virtual (unoccupied) orbitals, their eigenvalues and respective orbital symmetries are:

(-0.02491 A_1 LUMO) (-0.00398 A_1) (0.00844 B_2).

There is nothing remarkable about most of the MOs of the disiloxane molecule, except for MOs 13 to 16 shown in Figure 8, which could contribute to the opening of the Si-O-Si angle. This is especially true for MO 16 (-0.43954 B_2) of disiloxane, which is similar to the following MOs of octahydridosilasequioxane *inter alia* contributes to the formation of the MOs in its central cavity, namely; (-0.48780 A_{1g} MO 77) (-0.45870 F_{1u} MO 78-80) (-0.43496 E_g MOs 81,82) (-0.42532 F_{2g} MOs 83-85) (-0.42312 F_{1u} MOs 86-88) of which one member of each degenerate set of modes (except for MOs 81 and 82, but they look similar to the others) is shown in Figure 12; the MO energies are given in hartree.

6.2 Octahydridosilasequioxane O_h

The total molecular energy of the fully-optimized free molecule at its potential minimum is $E(\text{RB+HF-LYP}) = -3225.36229216$ hartree and it converged to within 0.8891×10^{-09} hartree in double precision.

(June 22, 2010)

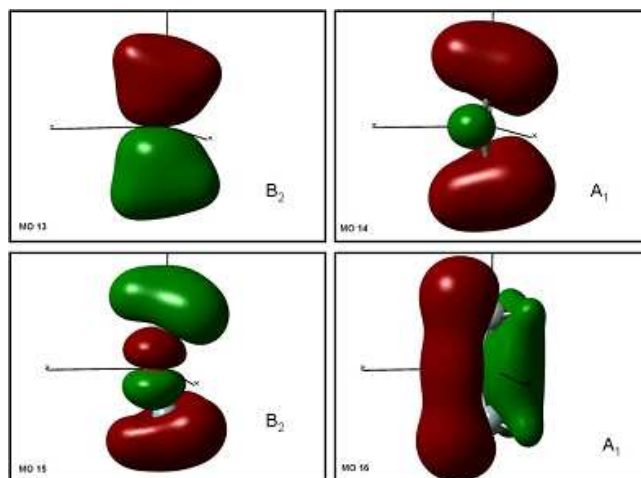


Figure 8: MOs 13 (top left), 14 (top right), 15 (bottom left) and 16 (bottom right) of the disiloxane molecule $\text{SiH}_3\cdot\text{O}\cdot\text{SiH}_3$.

6.2.1 Convergence criteria

The size of the computed virial-theorem ratio, that is, the negative ratio of the average potential and the kinetic energies, constitutes an important indication of the validity of any quantum mechanical calculation, especially for large molecules (Schutte 1976, p287f and references therein). For our optimization the virial ratio is found to be $-V/T = 2.0022$, which is sufficiently close to the ideal value of 2.0000 to give credence to the calculation. However, it is pointed out that the fulfillment of the virial ratio by any *ab-initio* calculation is a *necessary*, but not *sufficient condition* for the accuracy of any computed wave functions and their respective energies. The following convergence parameters were used (in atomic units), while the threshold values are given in brackets: *Maximum force* at converged geometry is 0.000034 (0.000450); *RMS force* 0.000009 (0.000300); *Maximum displacement* 0.000099 (0.001800); and *RMS displacement* 0.000027 (0.001200). The convergence obtained in this case is thus better than the limits imposed by the threshold values of the program.

6.2.2 MO energies and symmetries

The symmetries of the 108 doubly occupied bonding molecular orbitals and the first four antibonding (unoccupied) orbital sets of the optimized free octahedral molecule of octahydridosilasequioxane in order of decreasing negative energy, are as follows, listing only one member of each degenerate set:

Occupied:

(-66.16721 A_{2u})(-66.16721 F_{2g})(-66.16720 F_{1u})(-66.16720 A_{1g})(-19.13927 F_{2u})(-19.13927 E_g)
(-19.13927 F_{2g})(-19.13926 F_{1u})(-19.13925 A_{1g})(-5.33030 A_{2u})(-5.33030 F_{2g})(-5.33028 F_{1u})

(June 22, 2010)

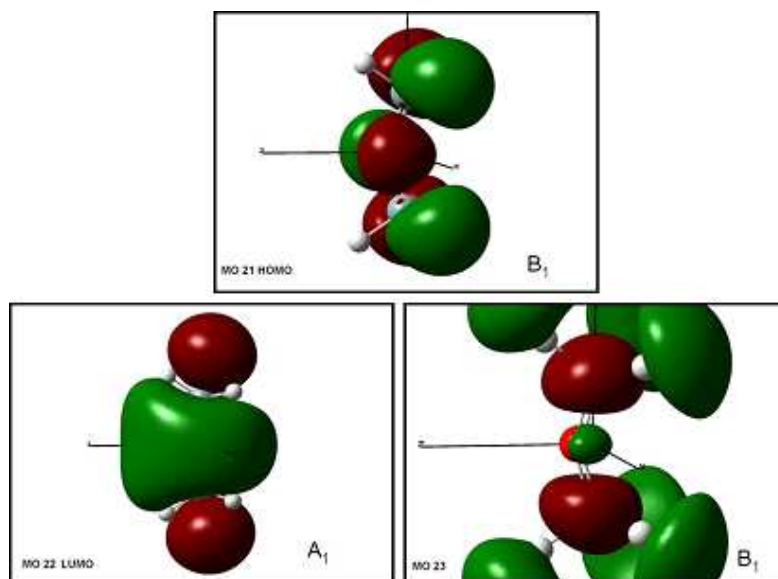


Figure 9: MOs 21 (top, HOMO), 22 (bottom left, LUMO) and 22 (bottom right, virtual orbital) of disiloxane.

(-5.33028 A_{1g})(-3.69 013 E_g)(-3.69013 F_{1u})(-3.69013 F_{2u})(3.69013 F_{2g})(3.69013 F_{1g})
 (-3.69013 E_u)(3.68754 A_{1g})(-3.68753 F_{1u})(-3.68751 F_{2g})(-3.68750 A_{2u})(-1.05882 A_{1g})
 (-1.04002 F_{1u})(-1.01904 F_{2g})(-0.99791 E_g)(-0.99680 F_{2u}) *** (-0.66276 A_{2u}) (-0.61968 F_{2g})
 (-0.57776 F_{1u})(-0.52057 F_{1g})(-0.51269 E_u)(-0.48780 A_{1g})(-0.45870 F_{1u})(-0.43496 E_g)
 (-0.42532 F_{2g})(-0.42312 F_{1u})(0.40318 A_{1g})(-0.37765 A_{2u})(-0.37649 F_{1g})(-0.37612 F_{2u})
 (-0.36309 E_g)(-0.35610 F_{1u})(-0.35161 F_{2g})(-0.35082 F_{2u})(-0.32292 A_{2g})

Virtual:

(-0.00942 A_{1g}) (0.00813 F_{1u}) (0.01324 A_{1g}) (0.01724 F_{2g}) (0.01887 E_g) ...

The 64 MOs belonging to the representation $(8A + 4E + 16F)$, dropping the subscripts, listed above are mostly almost pure slightly-perturbed AOs of the contributing Si and O atoms. The lowest occurs at (-66.16721 A_{2u}) and the list continues upwards to the triple asterisk *** to the right of (-0.99680 F_{2u}); this situation is similar to those shown above for the disiloxane molecule.

The 44 MOs starting to the right of the triple asterisk *** at (-0.66276 A_{2u}) up to the HOMO at (-0.32292 A_{2g}) are proper MOs, in many of which the hydrogen AOs play an important role. These MOs are further analyzed below. HOMO (Nr. 108) has A_{2g} and the LUMO (Nr. 109) A_{1g} symmetry; while the electronic ground state is $^1A_{1g}$. The energy difference between the HOMO and the LUMO of octahydridosilasequioxane orbitals is found to be $E_{(LUMO)} - E_{(HOMO)} = 0.3135$ hartree = $68805.30 \text{ cm}^{-1} = 823.09 \text{ kJ mol}^{-1} = 8.53 \text{ eV}$. This should be compared with that found by this study for SiH_4 with electronic state 1A_1 and disiloxane (C_{2v} with electronic state 1A_1), with energy values in hartree: SiH_4 : HOMO(-0.35529 F_2), LUMO(-0.00486 A_1), $E_{(LUMO)} - E_{(HOMO)} = 0.35043$ hartree, and $\text{SiH}_3\cdot\text{O}\cdot\text{SiH}_3$: HOMO(-0.31381

(June 22, 2010)

B_1), LUMO (-0.02491 A_1), $E_{(LUMO)} - E_{(HOMO)} = 0.2889$ hartree. This means that the LUMO-HOMO energy difference of octahydridosilasequioxane falls in the range computed for similar Si-compounds, although it is marginally larger than that computed for $\text{SiH}_3 \cdot \text{O} \cdot \text{SiH}_3$.

The classification of the molecular orbitals (MOs) of the molecule is important for the understanding of the electronic structure of the molecule, and a first classification is arrived at by comparing the energies of the MOs listed above with the ground state energies of the individual atomic orbitals (AOs) of the atoms constituting the molecule (computed using the same G03-methodology and bases sets), as well as by the shapes of the computed orbitals of the equilibrium molecular geometry as discussed below.

Eight Si-atoms contribute 112 electrons from the following *atomic orbitals*: $8(1s^2) = 16e$, $8(2s^2) = 16e$, $8(2p^6) = 48e$, $8(3s^2) = 16e$ and $8(3p^2) = 16e$. Twelve O-atoms contribute to 96 electrons in total from the following *atomic orbitals*: $12(1s^2) = 24e$, $12(2s^2) = 24e$, $12(2p^2) = 24e$. Eight H-atoms contribute 8e in total from the one orbital, *viz.* $8(1s^1) = 8e$.

The total number of electrons (216) is built up from individual AOs that form 108 occupied MOs. The hydrogen atoms contribute only eight electrons to the total of 216 electrons in the molecule (that is, they constitute less than 4% of the electron number), yet, as we showed above, the charges on them contribute largely to the properties of the molecule, as well as to the type of crystal packing of the individual molecules in the unit cell. A comparison of energies of the MOs listed above at the equilibrium structure of the octahydridosilasequioxane, $\text{Si}_8\text{H}_8\text{O}_{12}$ molecule and the computed energies and symmetries for the AOs of the constituting atoms immediately yields the following information regarding the relevant set of MOs (G03 computed MO symmetries and energies in hartree are listed in round brackets):

1. Occupied MOs remaining almost pure AOs:

- (a) MOs 1 to 8: (-66.16721 A_{2u}) (-66.16721 F_{2g}) (-66.16720 F_{1u}) (-66.16720 A_{1g}); 16e in 8 almost pure Si $1s^2$ AOs at -66.14313.
- (b) MOs 9 to 20: (-19.13927 F_{2u}) (-19.13927 E_g) (-19.13927 F_{2g}) (-19.13926 F_{1u}) (-19.13925 A_{1g}); 24e in 12 almost pure O $1s^2$ AOs at -19.27791.
- (c) MOs 21 to 28: (-5.33030 A_{2u}) (-5.33030 F_{2g}) (-5.33028 F_{1u}) (-5.33028 A_{1g}); 16e from 8 almost pure Si $2s^2$ AOs -5.30865.
- (d) MOs 29 to 52: (-3.69013 E_g) (-3.69013 F_{1u}) (-3.69013 F_{2u}) (3.69013 F_{2g}) (3.69013 F_{1g}) (-3.69013 E_u) (3.68754 A_{1g}) (-3.68753 F_{1u}) (-3.68751 F_{2g}) (-3.68750 A_{2u}); 48e in 24 almost pure Si $2p^6$ AOs at -3.67014 -3.66687 -3.66687.
- (e) MOs 53 to 64: (-1.05882 A_{1g}) (-1.04002 F_{1u}) (-1.01904 F_{2g}) (-0.99791 E_g) (-0.99680 F_{2u}); 24e in 12 almost pure O $2s^2$ AOs at -1.02487.

These five kinds of MOs are not further considered here, since they can be described as somewhat perturbed AOs, just about retaining their unperturbed AOs shapes, although their energies are a little bit shifted from those respective energies in the free atoms. There is no hydrogen AOs contribution in this group of orbitals.

2. Occupied orbitals forming proper MOs:

(June 22, 2010)

(a) MOs 65 to 108:

There are 88 electrons in 44 doubly occupied MOs from the outer shell AOs of:
(-0.66276 A_{2u} MO 65) (-0.61968 F_{2g} MOs 66-68) (-0.57776 F_{1u} MOs 69-71)
(-0.52057 F_{1g} MOs 72-74) (-0.51269 E_u MOs 75,76) (-0.48780 A_{1g} MO 77) (-
0.45870 F_{1u} MOs 78-80) (-0.43496 E_g MOs 81,82) (-0.42532 F_{2g} MOs 83-85)
(-0.42312 F_{1u} MOs 86-88) (0.40318 A_{1g} MO 89) (-0.37765 A_{2u} MO 90) (-0.37649
 F_{1g} MOs 91-93) (-0.37612 F_{2u} MOs 94-96) (-0.36309 E_g MOs 97,98) (-0.35610
 F_{1u} MOs 99-101) (-0.35161 F_{2g} MOs 102-104) (-0.35082 F_{2u} MOs 105-107) (-
0.32292 A_{2g} ; HOMO, MO 108).

These MOs are the proper molecular orbitals of the LCAO theory and will be discussed below, together with their orbital electron density plots (colloquially called "orbital shapes").

3. Antibonding or unoccupied orbitals:

(a) (-0.00942 A_{1g} LUMO, MO 109) (0.00813 F_{1u}) (0.01324 A_{1g}) (0.01724 F_{2g})...

These orbitals are important for the reactivity of the molecule and are further discussed below.

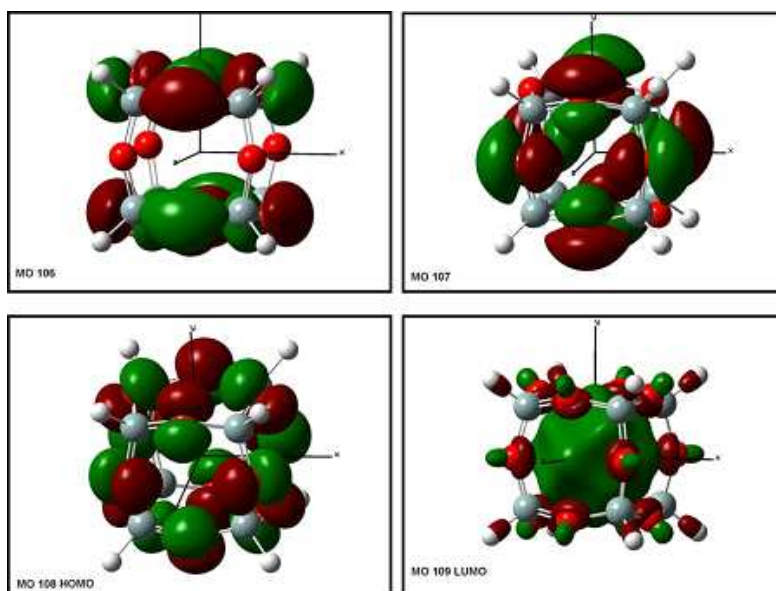


Figure 10: Electron-density diagrams of the highest orbitals, namely, MOs 106, 107, 108 (HOMO) & 109 (LUMO) of the octahydridosilasequioxane molecule. In these and the following diagrams the z -axis always points out of the paper, while x -axis points upwards and the y -axis to the right.

6.2.3 The orbital diagrams

Electron-density diagrams of MOs 106, 107, 108 (HOMO) and 109 (LUMO) of the octahydridosilasequioxane molecule are shown in Figure 10. *It is important*

(June 22, 2010)

to notice that neither the hydrogen atoms nor the silicon atoms take part in the MO-formation in the three highest bonding orbitals, that is, the accumulation of a partial negative electronic charge on the hydrogens comes from deeper-lying orbitals MOs 102-104 (see Figure 11, for instance); this fact might also contribute to the non-reactivity of the molecule. The energy difference between MO 102 and the HOMO is $0.02869 \text{ hartree} = 6296.7 \text{ cm}^{-1} = 70.31 \text{ kJ mol}^{-1} = 426.27 \text{ eV}$; this is quite large and might explain the fact why the molecule reacts readily in a high-temperature CVD process to deposit SiO_2 films (Nyman *et al.* 1993).

The shape of the LUMO (one of the frontier orbitals, MO 109, see Figure 10) displays almost no electron density on the outside of the cube for approaching electrophilic groups to interact with; in fact, the virtual electron density is accumulated in the centre of the cube. On the other hand, the absence of any electron density on the LUMO on the outside of the cube makes it easy for a nucleophilic group to approach, although the total partial negative charge that accumulated on the protruding hydrogen atoms may prevent this from happening. The "bareness" of the LUMO thus underlines the fact the molecule is rather unreactive at lower temperatures, although it might be used in the CVD-process to precipitate films of SiO_2 (Nyman *et al.* 1993), as mentioned above. The first virtual orbital that shows evidence of a virtual electron aggregation is MO 110, with the huge lobes in the y -direction that cover the two opposite faces of the cube.

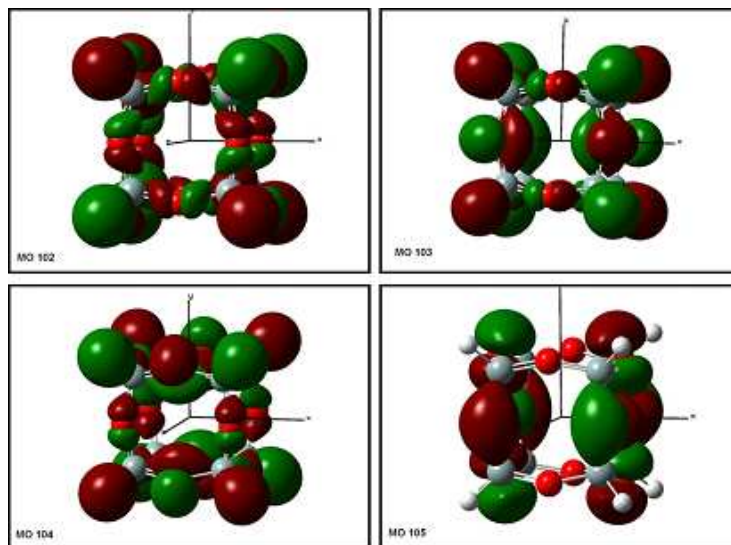


Figure 11: Electron-density diagrams of MOs 102 (top left), 103 (top right), 104 (bottom left) and 105 (bottom right).

MOs 102 to 106 are shown in Figure 11. MOs 102 to 104 clearly show the involvement of all the atoms in the MO formation, including the hydrogen atoms, while MO 105 at the right bottom involves only oxygen orbitals. There

(June 22, 2010)

is nothing spectacular in these MOs (or for that matter, in any of the other bonding MOs listed above, except for the four shown in Figure 10 and the one in Figure 11) that indicate any specific bonding effect that may be present, except for the fact that they offer an explanation why the molecule is unreactive, as explained above. However:

1. The sets of orbitals of MOs 77 to 88 form an interesting group, since they contribute to the opening tendency of the Si-O-Si angle, a fact already mentioned in the discussion about MO 16 of disiloxane above.
2. Figure 12 displays MOs 77 (top left), 80 (top right), 82 (bottom left) and 88 (bottom right). One set of orbitals, namely the triply-degenerate set (-0.42532 F_{2g} MOs 83-85) is not shown in the illustration, but MO 83 is displayed in Figure 13. These MOs are the only ones that show evidence of *electron density in the central cavity and on the faces of the cube*. The full set of such orbitals (with energies in hartree) is: (-0.48780 A_{1g} MO 77) (-0.45870 F_{1u} MOs 78-80) (-0.43496 E_g MOs 81, 82) (-0.42532 F_{2g} MOs 83-85) (-0.42312 F_{1u} MOs 86-88). One member of each degenerate set of MOs (except for MOs 81 and 82, but they look similar to the others) is shown in Figure 12
3. MO 83 looks different to the other members of the triply-degenerate set shown in Figure 13, since the -O- parts on its two opposite faces are on the inside and just about forms a kind of bent cylinder of charge that tends to make the bonding sequence more "straight", that is, it contributes as much to the bending-open of the Si-O-Si angle as the others. In any case, it must be remembered that the orbital wave functions of a triply-degenerate set are not unique, since any linear combination of them is also a valid orbital wave function (Schutte 1976). This means that a linear combination can be found that transforms MO 83 into a new function of which the electron distribution will look similar to that of MO 84 and 85 of the same set. These orbitals can be considered to be responsible for the opening of the Si-O-Si angles on the edges to about 144° . This molecule may be amenable to endo-substitution, such as by a Li^+ or H^+ ion.

6.3 Partial electron charges

The *partial electron charges*, q , on the atoms in the free molecule were computed with the G03 suite of programs as described above, using the *Mulliken* (Mulliken 1955) and *Atomic Polar Tensor* (APT) (Cioslowski 1989) models, yielding the results also included in Table 2. The Mulliken approach sometimes breaks down for bases functions containing diffuse functions (Baker 1985). As *reference points* the q_{H} , q_{Si} and q_{O} values for the isolated free gaseous molecules SiH_4 and $\text{H}_3\text{Si}\cdot\text{O}\cdot\text{SiH}_3$ discussed above were computed, using the same level of approximation.

A hydrogen atom attached to a Si atom in the reference compounds SiH_4 and $\text{H}_3\text{Si}\cdot\text{O}\cdot\text{SiH}_3$ is found to carry a negative computed Mulliken electron charge

(June 22, 2010)

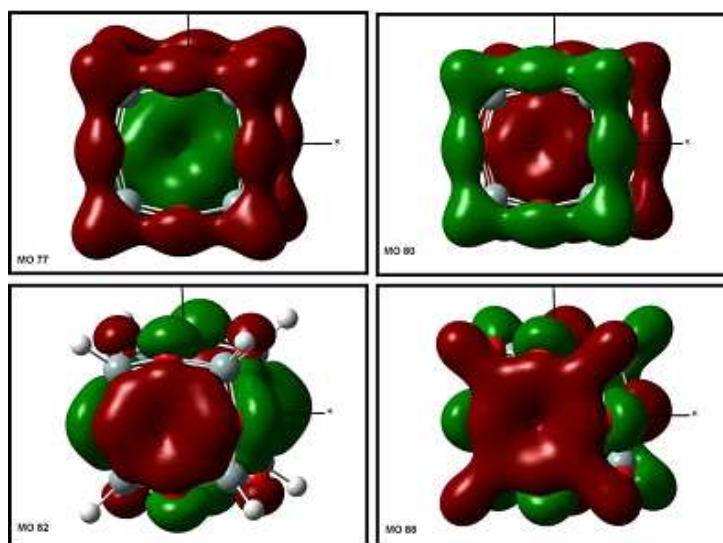


Figure 12: MOs 77 (top left), 80 (top right), 82 (bottom left) and 88 (bottom right) are the only MOs that show electron density in the central cavity and on the faces.

of around $-0.1e$ to $-0.13e$ (or an APT charge of around $-0.25e$). In octahydridosilasequioxane the Mulliken electron charge on the hydrogen atom is somewhat more negative, namely, $-0.18e$, but the APT charge is identical to those in the reference compounds, namely $-0.25e$. These *negatively-charged hydrogen atoms* in the free octahedral octahydridosilasequioxane molecule protrude radially from the surface of the free molecule, as it were, enveloping it in a cloud of negative electricity.

The *geometry* of the optimized free molecule is not significantly different from that found experimentally in the solid state; hence it can be concluded that a similar electron charge pattern would probably be found in the solid state. This enveloping halo of negative point charges offers an explanation for the packing pattern of the molecules in the unit cell, for the triangular plane formed between negatively-charged hydrogen atoms between two molecules as described above, as well as for the relative chemical non-reactivity of the solid compound. The molecule thus presents an almost perfectly repelling Faraday cage of negative surface electricity to any approaching molecule or group, especially if it is of the nucleophilic type. The same would apply to any other approaching octahydridosilasequioxane molecule: it would be repelled and there would be no opportunity for water to be eliminated between the two molecules to form typical silicate lattices.

Table 2 shows that the *bridging* negatively-charged oxygen atoms on the 12 edges of the $\text{Si}_3\text{H}_8\text{O}_{12}$ octahedron each carry a Mulliken charge of around $-0.38e$ (or a large APT charge of $-1.22e$). Each of the silicon atoms forming the octa-

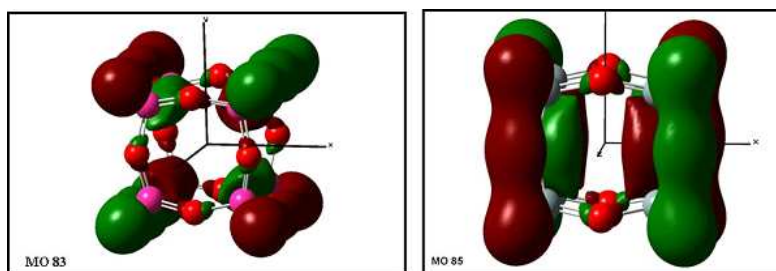


Figure 13: Two of the members of the triply-degenerate set ($-0.42532 F_{2g}$ MOs 83-85) that also contribute to the electron density in the central cavity. See the discussion in the text dealing with triply-degenerate wave functions.

hedral apices carries a positive Mulliken charge of $0.78e$ (or a very large $2.08e$ APT charge). If we compare the Mulliken and APT respective electron charges with the experimentally-obtained electron charges cited above for a magnesium silicate ($\text{Mg}_2[\text{SiO}_3]_2$), it is clear that the APT atomic charges on the *bridging* O and apex Si atoms of octahydridosilasequioxane approximate those of the experimental electron densities in magnesium silicate, very closely, namely: $\text{Mg} = +1.82e$, $\text{Si} = +2.28e$, $\text{O}_{\text{terminal}} = -1.42e$ and $\text{O}_{\text{bridging}} = -1.27e$ (see Table 1). This again exemplifies the validity of this type of computation, and, especially, it shows that in silica-type compounds, the APT densities present a better description of the theoretically calculated electron distribution than the Mulliken densities and that they closely approximate those found crystallographically in this case.

7 Conclusions

The results of this computational study allow us to reach the following conclusions, which are not only important for octahydridosilasequioxane, but also for silicate structures in general:

1. The all-electron GAUSSIAN G03 computed structure of the optimized free molecule confirms that it can be described by the molecular point group O_h , as shown in Figure 1.
2. The computed optimized geometrical O_h structure of the free molecule octahydridosilasequioxane is very near to that determined crystallographically by Törnroos (1994), except that the crystal is somewhat distorted in the unit cell by packing forces (the origin of which is discussed below), reducing the site symmetry to $C_{3i} = S_6$. Attention is especially drawn to the fact that there are two different Si-O bond lengths in the crystal emanating from the same silicon atom. The difference between the bond lengths is larger than the least-squares error of the bond-length determi-

nation of Törnroos (1994) and might be attributed to the novel packing situation of the molecules in the crystal as discussed below.

3. The computed Si-O-Si interbond angle of the free octahydridosilasequioxane molecule agrees with that found experimentally by Törnroos (1994). This is an indication that the computational procedure described here succeeds in modeling the structures of three-dimensional cyclic silicates of the type -Si-O-Si- quite well. However, for the free C_{2v} molecule disiloxane the Si-O-Si angle does not optimize that well, since it is predicted to be about 6° larger than the experimental value (see Table 2). There is no lattice to constrain the opening of the Si-O-Si angle in the optimization of this kind of molecule and the partial charges developing on the *three* hydrogen atoms in the silyl groups are thus, as it were, allowed by the optimization to "push open" the bond angle in contrast to the constraining effects in a lattice.
4. The packing of the octahydridosilasequioxane molecules in the lattice is interesting, and a thorough analysis of this aspect of the structure of the molecule uncovered an unsuspected packing scheme described here for the first time. This packing is illustrated in Figures 5 and 6 in which the apex H-atoms of eight octahydridosilasequioxane molecules take part. This packing arrangement is such that each apex H-atom of a protruding S-H bond of any octahydridosilasequioxane molecule points to the centre of an *equilateral* triangle having 2.631 Å sides; the triangle apices are formed by three apex atoms of three different other (partial) octahydridosilasequioxane molecules in the unit cell. The surfaces of the triangles at each apex end of a molecule are parallel to one-another and also parallel to the *ab*-plane, but the two triangles are rotated by 60° with respect to one-another. This packing arrangement of the two triangles, which, in perpendicular projection, looks similar to the Star of David, thus belongs to the symmetry point group $C_{3i} = S_6$. This packing thus determines the symmetry of the site group of the molecule in the lattice as described in the text and thus also the symmetry of the unit cell. A theoretical treatment of this packing arrangement in octahydridosilasequioxane and its relationship to the negative partial charges on all the participating hydrogen atoms (see the next points) will be published elsewhere.
5. The APT Si, O and H partial atomic electron densities computed here for the free octahydridosilasequioxane molecule agree with those obtained crystallographically for MgSiO_3 (Sasaki *et al.* 1982; for a discussion on accurate X-ray and neutron diffraction electron density and structural data for ortho-enstatite, MgSiO_3 , sometimes written as $\text{Mg}_2(\text{SiO}_3)_2$. It seems that the APT densities are far more useful for silicate work than the Mulliken densities. The computed partial charges on the atoms in the free octahydridosilasequioxane molecule show that H-atoms protruding from the Si-atoms from the ball of Si-O-Si bonds along the edges of a cube are all negative ($\sim 0.25e$, APT charges). This means that the octahedral

(June 22, 2010)

molecule presents a layer of negative charges to any approaching molecule. Since the geometric structure of the octahydridosilasequioxane molecule in the solid state differs very little from that of the free molecule, there is little or no reason to believe that the partial charges on its atoms would be considerably different. That this conclusion is warranted is shown by the optimization results on a "stand-alone" specially-designed cluster of eight octahydridosilasequioxane molecules in the solid state configuration. The individual molecules do not disperse as the optimization proceeded (as is often the case when there are no specific pairs of attractive centers, such as hydrogen bonds), but seem to be glued closely together by the same triangle of hydrogen atoms and the same configuration around it as described in the text (see Figures 5 and 6) - even though the hydrogen atoms show the same partial negative charges.

6. The computation of all 108 molecular orbital electron densities plus some orbitals belonging to the LUMO and other virtual orbitals of octahydridosilasequioxane, allowed us to conclude that a number of MOs exist (MOs 77 to 88; see Figures 12 and 13), which allow some electron density to accumulate in the central cavity of the cube. This in turn, most probably contribute to the forces that open up the Si-O-Si bonds from the ideal tetrahedral angle of $\sim 109^\circ$. All these modes are conceptually derived from MO16 of the "monomer unit", disiloxane (see Figure 8), which also contributes to the opening up of the Si-O-Si angle.
7. The LUMO-HOMO gap of octahydridosilasequioxane is in the range of gaps observed for similar molecules.
8. The shape of the LUMO (MO 109, Figure 10) shows hardly any electronegativity on the outside of the cube for approaching electrophilic groups to interact with; in fact, the virtual electron density is accumulated in the centre of the cube. On the other hand, the absence of any electron density on the LUMO on the outside of the cube makes it easy for a nucleophilic group to approach, although the total partial negative charge that accumulated on the protruding hydrogen atoms may prevent this from happening. It thus seems that the molecule is rather unreactive, although it might be used in the CVD-process to precipitate films of SiO₂ (Nyman *et al.* 1993)

Acknowledgements

We express our appreciation for the use of the IBM Computer Cluster at the University of Pretoria, supported by PBMR (Pty) Ltd. (<http://www.pbmr.co.za>).

Agaskar P.A. (1991) New Synthetic Route to the hydridospherosiloxanes O_h -H₈Si₈O₁₂ and D_{5h} -H₁₀Si₁₀O₁₅. *Inorg. Chem.* **30**:2707-2708.

Agaskar P.A., Klemperer W. (1995) The higher hydridospherosiloxanes: synthesis and structures of H_nSi_nO_{1.5n}, ($n = 12, 14, 16, 18$). *Inorg. Chim. Acta* **229**:355-364.

(June 22, 2010)

- Almenningen A., Bastiansen O., Ewing V., Hedberg K., Traetteberg M. (1963) The molecular structure of disiloxane, $(\text{SiH}_3)_2\text{O}$. *Acta Chem. Scand.* **17**(9):2455-2460.
- Almenningen A., Bjorvatten T. (1963) An electron diffraction investigation of the structure of antimony triiodide. *Acta Chem. Scand.* **17**(9):2573-2574.
- Aronson J.R., Lord R.C., Robinson D.W. (1960) Far Infrared Spectrum and Structure of Disiloxane. *J. Chem. Phys.*, **33**:1004-1007. *See erratum:* (Aronson, Lord & Robinson, 1961).
- Aronson J.R., Lord R.C., Robinson D.W. (1961) Far Infrared Spectrum and Structure of Disiloxane. *J. Chem. Phys.* **35**:2245.
- Bailar Jr J.C., Emeléus H.J., Nyholm R., Trotman-Dickenson A.F. (1973) Comprehensive Inorganic Chemistry. **Vol. 1**, Pergamon Press, Oxford, U.K., p.1469 ff.
- Baker J. (1985) Classical chemical concepts from ab initio SCF calculations. *Theor. Chim. Acta* **68**(3):221-229.
- Bilinski H, Horvath L and Trbojevic-Cepe M. (1992) Precipitation and Characterization of an Aluminosilicate from $\text{AlCl}_3\text{-Na}_2\text{SiO}_3\text{-HCl}$ in Serum, of interest for Alzheimer Disease. *Clin. Chem.* 38/10:2019-2024.
- Birchall J.D. and Chappell J.S. (1988) The Chemistry of Aluminum and Silicon in Relation to Alzheimer's Disease. *Clin. Chem.* 34/2:265-267.
- Boeyens J.C.A. (2008) The Periodic Electronegativity Table. *Z. Naturforsch.* **63b**:199-209.
- Cioslowski J.J. (1989) A new population analysis based on atomic polar tensors. *J. Am. Chem. Soc.* **111**(22):8333-8336.
- Cotton F.A., Wilkinson G. (1988) Advanced Inorganic Chemistry. *John Wiley & Sons, New York*, **5th Edition**, p.274ff.
- Csonka G.I., Réffy J. (1994) Density functional study of the equilibrium geometry and Si-O-Si potential energy curve of disiloxane. *Chem. Phys. Lett.* **229**:191-197.
- Dusek M., Petricek W., Wuenschel M., Dinnebier R.E., van Smaalen S. (2001) Refinement of modulated structures against X-ray powder diffraction data with JANA2000. *J. Appl. Crystallogr.* **34**(3):398-404, ICSD#93093.
- Foresman J.B., Frisch \AA . (1998) Exploring Chemistry with Electronic Structure Methods. **2nd Edition**. *Gaussian Inc. Pittsburgh PA, USA*.
- Frisch M.J. and Nielsen A.B., Edited by Frisch \AA . and Trucks G.W. (2003) Gaussian 03 Programmers Reference. *Gaussian, Inc., Wallingford, CT 06492, U.S.A.*, (info@gaussian.com).
- GaussView**: Dennington R (II), Keith T., Millam J. (2007) **Version 4.1**, *Semichem., Inc., Shawnee Mission, KS*.
- Gaussian 03: Rev. C.02** (2004) Frisch M.J., Trucks G.W., Schlegel H.B., Scuseria G.E., Robb M.A., Cheeseman J.R., Montgomery J.A. Jr., Vreven T., Kudin K.N., Burant J.C., Millam J. M., Iyengar S.S., Tomasi J., Barone V., Mennucci B., Cossi M., Scalmani G., Rega N., Petersson G.A., Nakatsuji H., Hada M., Ehara M., Toyota K., Fukuda R., HasEgawa J., Ishida M., Nakajima T., Honda Y., Kitao O., Nakai H., Klene M., Li X., J, Knox. E., Hratchian H.P., Cross J.B., Bakken V., Adamo C., Jaramillo J., Gomperts R.,

(June 22, 2010)

Stratmann R.E., Yazyev O., Austin A.J., Cammi R., Pomelli C., Ochterski J.W., Ayala P.Y., Morokuma K., Voth G.A., Salvador P., Dannenberg J.J., Zakrzewski V.G., Dapprich S., Daniels A.D., Strain M.C., Farkas O., Malick D.K., Rabuck A.D., Raghavachari K., Foresman J.B., Ortiz J.V., Cui Q., Baboul A.G., Clifford S., Cioslowski J., Stefanov B.B., Liu G., Liashenko A., Piskorz P., Komaromi I., Martin R.L., Fox D.J., Keith T., Al-Laham M.A., Peng C.Y., Nanayakkara A., Challacombe M., Gill P.M.W., Johnson B., Chen W., Wong M.W., Gonzalez C., Pople J.A. *Gaussian Incorporate, Wallingford CT*. (See also <http://www.gaussian.com>).

Hahn T. [Editor](1987) International Tables for Crystallography. Volume A, Space-group Symmetry. Second Revised Edition. (Trigonal Space Group 148, $R\bar{3}$, C_{3i}^2) pp. 498).

Heyl D., Rikowski E., Hoffman R.C., Schneider J.J. and Fessner W-D. (2010) A “Clickable” Hybrid Nanocluster of Cubic Symmetry. *Chem. Eur. J.* **16**:5544-5548.

Hirst D.M. (1990) A Computational Approach to Chemistry. *Blackwell Scientific Publications, Oxford, UK*.

Knight T.G., Kirkpatrick R.J., Oldfield E. (1986) Silicon-29 NMR Structural Characterization of Two Novel Germanosilicate Cages in a Tetramethylammonium Germanosilicate Solution. *J. Am. Chem. Soc.* **108**:30.

Kohanoff J. (2006) Electronic Structure Calculations for Solids and Molecules. Theory and Computational Methods. *Cambridge University Press, Cambridge, UK*.

Kresse G., Furthmüller J. (1996) Efficient iterative schemes for *ab initio* total-energy calculations using a plane-wave basis set. *Phys. Rev. B* **54**(16):11169-11186.

Kresse G., Furthmüller J. (1996) Efficiency of *ab-initio* total energy calculations for metals and semiconductors using a plane-wave basis set. *Comp. Mat. Sci.* **6**(1):15-50.

Kresse G., Joubert D. (1999) From ultrasoft pseudopotentials to the projector augmented-wave method. *Phys. Rev. B* **59**:1758.

Kuchitsu K.(Editor) (1998) Structure of Free Polyatomic Molecules. *Springer-Verlag, Berlin*, (pp.68 and 71, respectively).

Larsson K. (1960) The crystal structure of Octa-(silsesquioxanes), $(\text{RSiO}_{1.5})_8$ and $(\text{ArSiO}_{1.5})_8$. *Arkiv Kemi* **16**:209-214. ICSD#27154.

Lide A.D. Jr.(Editor) (2009-2010) Handbook of Chemistry and Physics. *CRC, Baton Rouge, 90th Edition*.

Liebau F. (1985) Structural Chemistry of Silicates. *Springer-Verlag, Berlin*.

Lord R.C., Robinson D.W., Schumb W.C. (1956) Vibrational Spectra and Structure of Disiloxane and Disiloxane- d_6^1 . *J. Am. Chem. Soc.* **78**:1327-1332.

Mak T.C.W., Zhou G.D. (1992) Crystallography in Modern Chemistry. A Resource Book of Crystal Structures. *John Wiley & Sons, Inc. New York*, p298ff. (α -quartz, p.97ff; $\text{Mg}_2[\text{SiO}_3]_2$, p145 and generalized details on silicate structures pp. p298, 299f).

McDonald W. S., Cruickshank D.W. J. (1967) A Reinvestigation of the Structure of Sodium Metasilicate Na_2SiO_3 . *Acta Crystallogr.* **22**:37.

(June 22, 2010)

MedeA: Materials Design and Exploration Analysis Software (Copyright 1998-2006). *Materials Design, Inc., Version 2.3.0.2*. MedeA Users' Guide, **Version 2**. *Theoretical Background* at the licensed software product web-site: <http://localhost:32000/Doc/index.htm>.

MedeA: Phonon software version 4.28 (2003) Copyright Prof. K. Parlinski: See K. Parlinski, Software Phonon <http://wolf.ifj.edu.pl/phonon/>.

MedeA: VASP software version 4.6.31 (2009), written in the Group of Prof. J. Hafner by G. Kresse and J. Furthmüller, from the Institut für Materialwissenschaft, Universität Wien.

Mercury: For details of the freely-distributed program, see the web site of the Cambridge Crystallographic Data Centre (CCDC) at www.ccdc.cam.ac.uk.

Morosin B. (1972) Structure and Thermal Expansion of Beryl. *Acta Crystallogr.* **B28**:1899.

Mulliken R.S. (1955) Electronic Population Analysis on LCAO - MO Molecular Wave Functions I. *J. Chem. Phys.* **23**:1833.

Mulliken R.S. (1955) Electronic Population Analysis on LCAO - MO Molecular Wave Functions II. *J. Chem. Phys.* **23**:1841.

Mulliken R.S. (1955) Electronic Population Analysis on LCAO - MO Molecular Wave Functions III. *J. Chem. Phys.* **23**:2338.

Mulliken R.S. (1955) Electronic Population Analysis on LCAO - MO Molecular Wave Functions IV. *J. Chem. Phys.* **23**:2343.

Needels M., Joannopoulos J.D., Bar-Yam Y., Pantelides S.T. (1991) Complexes in silicon. *Phys. Rev. B* **43**:4208.

Needels M., Joannopoulos J.D., Bar-Yam Y., Pantelides S.T. (1991) The enchanting properties of oxygen atoms in silicon. *Mat. Res. Soc. Symp. Proc.* **209(Defects Mat.)**:103-117.

Nyman M.D., Desu S.B., Peng C.H. (1993) T_s-Hydridospherosiloxanes: Novel Precursors for SiO₂ Thin Films. 1. Precursor Characterization and Preliminary CVD. *Chem. Mater.* **5**:1636-1640.

Origin 7.5 SR4: Software Version 7.5853 (B853), Origin Lab Corporation, One Roadhouse Plaza, Northampton MA 01060, USA. <http://www.OriginLab.com>.

Owen H., Tabak S.A. and Wright B.S. (1985) Process for converting olefins to gasoline, distillate and alkylate hydrocarbons. United States Patent: 4,633,037. Appl. No.: 06/779,373, Mobil Oil Corporation.

Pant A.K. (1968) A reconsideration of the crystal structure of β -Na₂Si₂O₅. *Acta Crystallogr.* **24**:1077.

Pauling L. (1960) The Nature of the Chemical Bond. *Oxford University Press*, **3rd Ed.**

Popović Z X., Sljivancanin Z.V., Vukaljović F.R. (2004) Sodium Pyroxene NaTiSi₂O₆: Possible Haldane Spin-1 Chain System. *Phys. Rev. Lett.* **93(3)**:036401/1-036401/4.

Sasaki S., Takuchi Y., Fujino K., Akimoto S. (1982) Electron distributions of three orthopyroxenes, Mg₂Si₂O₆, Co₂Si₂O₆ and Fe₂Si₂O₆. *Z. Kristallogr.* **158(3-4)**:279-97.

Schutte C.J.H. (1976) The Theory of Molecular Spectroscopy. **Vol. 1:** The Quantum Mechanics and Group Theory of Vibrating and Rotating Molecules,

(June 22, 2010)

North-Holland/American Elsevier, Amsterdam/New York.

Seddon D., (2006) Gas usage & value: The Technology and Economic of Natural Gas use in the Process Industries. *English book xv, Penwell, ISBN: 1593700733*

SUSE LINUX Enterprise SERVER Operating System, Version 10.2.

Streltsov S.V., Popova O.A., Khomskii D.I. (2006) Comment on "Sodium Pyroxene NaTiSi₂O₆: Possible Haldane Spin-1 Chain System". *Phys. Rev. Lett.* **96**:249701-2

Swanson D.K., Prewitt C.T. (1983) The crystal structure of potassium silicate K₂Si^{VI}Si₃^{IV}O₉. *Am. Miner.* **68**(5-6):581-5.

Taga K, Kawasaki K., Yamamoto Y., Yoshida T. Ohno K., Matsuura H. (2006) Raman spectra and conformational analyses for a series of diethyl ether and its organosilicon derivatives, CH₃MH₂OM'H₂CH₃ (M, M' = C and Si), by Density Functional Theory. *J. Mol Struct.* **788**(1-3):159-175.

Törnroos K.W. (1994) Octahydridosilasesquioxane Determined by Neutron Diffraction. *Acta Crystallogr.* **C50**:1646, ICSD#75244.

Tucker M.G., Keen D.A., Dive M.T. (2001) A detailed structural characterization of quartz on heating through the α - β phase transition. *Mineral. Mag.* **65**(4): 489-507. (ICSD#93975).

Vora B.V, Marker T.L., Barger P.T., Nilsen H.R., Kvisle S., Fuglerud T. (1997) Economic Route for Natural Gas Conversion to Ethylene and Propylene. *Stud. Surf. Sci. Catal.* **107**:87-98.

Wells A.F. (1984) Structural Inorganic Chemistry, **5th Ed.**, Clarendon Press, Oxford, p.1011ff.

Wilson S., Barger P. The Characteristics of SAPO-34 which influence the conversion of methanol to light olefins. *Microporous and Mesoporous Materials*, **29**(1-2):117-126

Wolfe R.H., Needels M., Joannopoulos J.D. (1991) The electronic structure of oxygen in silicon as revealed by volume visualization of ab initio calculations. *Proc. 2nd Conference on Visualization.*

Wright A.F., Lehmann M.S. (1981) The Structure of Quartz at 25 and 590°C determined by Neutron Diffraction. *Solid State Chem.* **36**:371-380.

(June 22, 2010)

TABLES

Table 1: Relevant bond and electron density properties of some silicates (Wright *et al.* 1981; Dusek *et al.* 2001; Mak *et al.* 1992; Tucker *et al.* 2001).

Name	$r(\text{Si-O})/\text{\AA}$	$\phi(\text{Si-O-Si})/^\circ$	$q(\text{Si})/e$	$q(\text{O})/e$	$q(\text{Mg})/e$
α -Quartz	1.608, 1.610	153.0	-	-	-
β -Quartz	1.58	169.0	1.22	-0.61	-
$\text{Mg}_2[\text{SiO}_3]_2$	1.588(6)	117.15(4)	2.28	-1.42 (Term.)	1.82
continued	1.612(6)	117.15(4)	-	-1.27 (Brid.)	-
continued	1.646(8)	127.98(4)	-	-	-
continued	1.665(7)	134.35(4)	-	-	-

(June 22, 2010)

Table 2: The DFT/B3LYP/6-311++G3df,3pd) basis set computed structural and electron density data for the O_h model of octahydridosilasequioxane. The APT electron density data are shown in brackets following the Mulliken electron densities. The Törnroos neutron diffraction geometric parameters are also included for purposes of comparison, as well as computed and experimental structural and electron density data. Distances are in Å, angles in degree, and electron density in fractions of an electron. e. The rhombohedral angles are $\alpha = \beta = 90^\circ$, $\gamma = 120^\circ$ for both the MedeA-computed and the experimental crystal structures. The unit cell dimensions of the MedeA-computed crystal structure are, respectively, 4.3, 4.3 and 4.5% larger than that of the experimentally-determined crystal structure (see discussion above).

	SiH ₄ T_d (G03 com- puted)	SiH ₄ (g) T_d exp. (Kuchitsu 1998)	H ₃ Si-O-SiH ₃ C_{2v} (G03 com- puted)	H ₃ Si-O-SiH ₃ exp. (g) (Kuchitsu 1998)	Si ₈ H ₈ O ₁₂ O_h (G03 Com- puted)	Si ₈ H ₈ O ₁₂ exp.* (Törn- roos 1994)	Si ₈ H ₈ O ₁₂ (MedeA- VASP com- puted*)
$re(\text{Si-H})$	1.480	1.4707	1.481	1.486	1.458	1.459	1.469
$re(\text{Si-H})$	1.480	1.4707	1.477	1.486	-	-	1.469
$re(\text{Si-H})$	1.480	1.4707	1.477	1.486	-	-	1.469
$re(\text{Si-O})$	-	-	1.638	1.634	1.629	1.626 1.623	1.639 -
$r(\text{O} \dots \text{O})$	-	-	-	-	3.768 3.768	3.927 3.546	3.833 3.646
$\langle \text{Si-O-Si} \rangle$	-	-	150.7	144.1	148.0	147.3, 147.5	153.4 160.9
$q\text{H}$	-0.12e (-0.24e)	-	-0.11e (-0.26)	-	-0.18 (-0.25)	-	-
$q\text{H}$	-	-	-0.13e (- 0.26e)	-	-	-	-
$q\text{H}$	-	-	-0.13e (- 0.26e)	-	-	-	-
$q\text{Si}$	0.46e (0.93e)	-	0.62 (??)	-	0.78 (??)	-	-
$q\text{O}$	-	-	-0.49e (- 1.29e)	-	-0.38 (-1.22)	-	-
a	-	-	-	-		9.0530	9.439
b	-	-	-	-		9.0530	9.439
c	-	-	-	-		15.1490	15.859

SUPPLEMENTARY MATERIAL

Verwysende teks in die artikel:

A comparison of energies of the AOs and MOs and their respective symmetries are available as supplementary material **Ref.1**.

Ref 1: MO's of the molecule Disiloxane

A comparison of energies of the MOs at the equilibrium C_{2v} -optimized structure of the octahydridosilasequioxane, $Si_8H_8O_{12}$ molecule and the computed energies and symmetries for the AOs of the separate constituting atoms Si, O and H immediately yields the following information regarding the lower set of MOs (G03 computed MO symmetries and energies in hartree are listed in round brackets):

(a) Occupied MOs remaining almost pure AOs:

1. **MOs 1 and 2:** (-66.12113 B₂) (-66.12113 A₁) 4e in almost pure Si 1s² AO at -66.14313 hartree
2. **MO 3:** (-19.12964 A₁) 2e in almost pure O 1s² AO at -19.27791 hartree
3. **MOs 4 to 5:** (-5.29109 B₂) (-5.29107 A₁) 4e from almost pure Si 2s² AO at -5.30865 hartree
4. **MOs 6 to 11:** (-3.65086 A₁) (-3.65085 B₂) (-3.64862 B₁) (-3.64862 A₂) (-3.64858 A₁) (-3.64857 B₂) 12e from the set of 12 Si 2p⁶ AOs at -3.67014, -3.66687, -3.66687 hartrees

(b) Occupied orbitals forming proper MOs:

5. **MOs 12 to 21:**

There are 18 electrons in 9 doubly occupied MOs from the outer shells AOs of Si, O and H at the following computed values:

[Si 3s² (-0.45591) + Si 3p² (-0.19417) + O 2p²(0.39164) + H 1s¹ (-0.50226)] giving rise to MOs at the following symmetries:
(-1.00400 A₁) (-0.60135 B₂) (-0.51057 A₁) (-0.43954 B₂) (-0.41702 A₁) (-0.41608 B₁)
(-0.35402 B₂) (-0.35353 A₂) (-0.31706 A₁) (-0.31381 B₁)

A huge decrease in energy is observed going from the respective AOs to the MOs, showing the extent of the electronic interaction when the MOs are formed. Hydrogen atoms play a large role in the MO-structure. These MOs are the proper molecular orbitals of the LCAO theory and are discussed below, together with their SCF orbital electron density plots (colloquially called "orbital shapes").

(c) **Virtual orbitals 22 - 24:**

The virtual (unoccupied) eigenvalues and their orbital symmetries are:
(-0.02491 A₁ LUMO) (-0.00398 A₁) (0.00844 B₂)

Verwysende teks in die artikel:

The symmetries of the 108 doubly occupied bonding molecular orbitals and the first four antibonding (unoccupied) orbital sets of the optimized free octahedral molecule of octahydridosilasequioxane, are listed in Supplementary Material **Ref. 2**.

Ref 2: MO's of the molecule Octahydridosilasequioxane O_h

The symmetries of the 108 doubly occupied bonding molecular orbitals and the first four antibonding (unoccupied) orbital sets of the optimized free octahedral molecule of octahydridosilasequioxane in order of decreasing negative energy, are as follows, listing only one member of each degenerate set:

Occupied: (-66.16721 A_{2u}) (-66.16721 F_{2g}) (-66.16720 F_{1u}) (-66.16720 A_{1g}) (-19.13927 F_{2u}) (-19.13927 E_g)
(-19.13927 F_{2g}) (-19.13926 F_{1u}) (-19.13925 A_{1g}) (-5.33030 A_{2u}) (-5.33030 F_{2g}) (-5.33028 F_{1u})
(-5.33028 A_{1g}) (-3.69 013 E_g) (-3.69013 F_{1u}) (-3.69013 F_{2u}) (3.69013 F_{2g}) (3.69013 F_{1g})
(-3.69013 E_u) (3.68754 A_{1g}) (-3.68753 F_{1u}) (-3.68751 F_{2g}) (-3.68750 A_{2u}) (-1.05882 A_{1g})
(-1.04002 F_{1u}) (-1.01904 F_{2g}) (-0.99791 E_g) (-0.99680 F_{2u}) *** (-0.66276 A_{2u}) (-0.61968 F_{2g})
(-0.57776 F_{1u}) (-0.52057 F_{1g}) (-0.51269 E_u) (-0.48780 A_{1g}) (-0.45870 F_{1u}) (-0.43496 E_g)
(-0.42532 F_{2g}) (-0.42312 F_{1u}) (0.40318 A_{1g}) (-0.37765 A_{2u}) (-0.37649 F_{1g}) (-0.37612 F_{2u})
(-0.36309 E_g) (-0.35610 F_{1u}) (-0.35161 F_{2g}) (-0.35082 F_{2u}) (-0.32292 A_{2g})
Virtual : (-0.00942 A_{1g}) (0.00813 F_{1u}) (0.01324 A_{1g}) (0.01724 F_{2g}) (0.01887 E_g)

The 64 MOs belonging to the representation (8A + 4E + 16F, dropping the subscripts) listed above are mostly almost pure slightly-perturbed AOs of the contributing Si and O atoms. The lowest occurs at (-66.16721 A_{2u}) and the list continues upwards to the triple asterisk *** to the right of (-0.99680 F_{2u}); this situation is similar to those shown above for the disiloxane molecule.

The 44 MOs starting to the right of the triple asterisk *** at (-0.66276 A_{2u}) up to the HOMO at (-0.32292 A_{2g}) are proper MOs, in many of which the hydrogen AOs play an important role. These MOs are further analyzed below. HOMO (Nr. 108) has A_{2g} and the LUMO (Nr. 109) A_{1g} symmetry; while the electronic ground state is $^1A_{1g}$.

Verwysende teks in die artikel:

A comparison of energies and symmetries of the MOs listed above at the equilibrium structure of the octahydridosilasequioxane, $Si_8H_8O_{12}$ molecule and the computed energies and symmetries for the AOs are referenced in Supplementary material **Ref 3**.

Ref 3: Comparison of energies and symmetries of the MO energies and symmetries at the equilibrium structure of the octahydridosilasequioxane $Si_8H_8O_{12}$ molecule

A comparison of energies of the MOs listed above at the equilibrium structure of the octahydridosilasequioxane, $Si_8H_8O_{12}$ molecule and the computed energies and symmetries for the AOs of the constituting atoms immediately yields the following information regarding the lower set of MOs (G03 computed MO symmetries and energies in hartree are listed in round brackets):

(a) Occupied MOs remaining almost pure AOs:

- (1) **MOs 1 to 8:** (-66.16721 A_{2u}) (-66.16721 F_{2g}) (-66.16720 F_{1u}) (-66.16720 A_{1g})
16e in 8 almost pure Si 1s² AOs at -66.14313
- (2) **MOs 9 to 20:** (-19.13927 F_{2u}) (-19.13927 E_g) (-19.13927 F_{2g}) (-19.13926 F_{1u}) (-19.13925 A_{1g})
24e in 12 almost pure O 1s² AOs at -19.27791
- (3) **MOs 21 to 28:** (-5.33030 A_{2u}) (-5.33030 F_{2g}) (-5.33028 F_{1u}) (-5.33028 A_{1g})
16e from 8 almost pure Si 2s² AOs -5.30865
- (4) **MOs 29 to 52:** (-3.69 013 E_g) (-3.69013 F_{1u}) (-3.69013 F_{2u}) (3.69013 F_{2g}) (3.69013 F_{1g})
(-3.69013 E_u) (3.68754 A_{1g}) (-3.68753 F_{1u}) (-3.68751 F_{2g}) (-3.68750 A_{2u})
48e in 24 almost pure Si 2p⁶ AOs at -3.67014 -3.66687 -3.66687
- (5) **MOs 53 to 64:** (-1.05882 A_{1g}) (-1.04002 F_{1u}) (-1.01904 F_{2g}) (-0.99791 E_g) (-0.99680 F_{2u})
24e in 12 almost pure O 2s² AOs at -1.02487

These MOs are not further considered here, since they can be described as somewhat perturbed AOs, just about retaining their unperturbed AOs shapes, although their energies are a little bit shifted from those respective energies in the free atoms. There is no hydrogen AOs contribution in this group of orbitals.

(b) Occupied orbitals forming proper MOs:

(6) MOs 65 to 108:

There are 88 electrons in 44 doubly occupied MOs from the outer shell AOs of:

- (-0.66276 A_{2u} MO 65) (-0.61968 F_{2g} MOs 66-68) (-0.57776 F_{1u} MOs 69-71)
(-0.52057 F_{1g} MOs 72-74) (-0.51269 E_u MOs 75,76) (-0.48780 A_{1g} MO 77)
(-0.45870 F_{1u} MOs 78-80) (-0.43496 E_g MOs 81,82) (-0.42532 F_{2g} MOs 83-85)
(-0.42312 F_{1u} MOs 86-88) (0.40318 A_{1g} MO 89) (-0.37765 A_{2u} MO 90)
(-0.37649 F_{1g} MOs 91-93) (-0.37612 F_{2u} MOs 94-96) (-0.36309 E_g MOs 97,98)
(-0.35610 F_{1u} MOs 99-101) (-0.35161 F_{2g} MOs 102-104) (-0.35082 F_{2u} MOs 105-107)
(-0.32292 A_{2g} HOMO, MO 108)

These MOs are the proper molecular orbitals of the LCAO theory and will be discussed below, together with their orbital electron density plots (colloquially called "orbital shapes").

(c) Antibonding or unoccupied orbitals

(7) Unoccupied MOs:

- (-0.00942 A_{1g} LUMO, MO 109) (0.00813 F_{1u}) (0.01324 A_{1g}) (0.01724 F_{2g})...

These orbitals are important for the reactivity of the molecule and will also be discussed below.